Date of publication xxxx 00, 0000, date of current version xxxx 00, 0000.

*Digital Object Identifier 10.1109/ACCESS.2020.DOI*

# Joint Beamforming and Power Allocation for Multiuser MISO Broadcast Channel SWIPT Employing OFDM

**RICHARD P. KETCHAM, (Student Member, IEEE), JEROEN VERDYCK, (Student Member, IEEE), AND MARC MOONEN, (Fellow, IEEE)**

KU Leuven, Department of Electrical Engineering (ESAT), STADIUS Center for Dynamical Systems, Signal Processing and Data Analytics, Leuven, Belgium

Corresponding author: Richard P. Ketcham (e-mail: Richard.Ketcham@kuleuven.be).

This research work was carried out at the ESAT Laboratory of KU Leuven, in the frame of: Fonds de la Recherche Scientifique - Fonds Wetenschappelijk Onderzoek - Vlaanderen EOS Project no 30452698 '(MUSE-WINET) MUlti-SErvice WIreless NETwork.' The scientific responsibility is assumed by its authors.

**ABSTRACT** A resource allocation algorithm is considered to optimize beamforming vectors and power allocation in a multiuser (MU) multiple-input single-output (MISO) broadcast channel (BC) simultaneous wireless information and power transfer (SWIPT) system that employs orthogonal frequency division multiplexing (OFDM). A non-convex optimization problem is formulated in which a weighted sum of user data rates is maximized subject to meeting received power and transmit power constraints. The algorithm exploits the time-sharing property of multicarrier systems to overcome this non-convexity and enables utilizing Lagrangian decomposition to parallelize the problem. Further simplification is achieved via a multiple access channel (MAC) - BC duality, which enables a closed-form solution for the beamforming vectors given the dual MAC power allocation. The dual MAC power allocation is approximated using a successive convex approximation (SCA) technique. The resulting algorithm jointly optimizes beamforming vectors and power allocation in a MU-MISO-BC-SWIPT system employing OFDM that provides close-to-optimal performance without relying on subcarrier assignment at significantly lower computational complexity than comparable algorithms.

**INDEX TERMS** MAC-BC, MISO, Multiuser, OFDM, Optimization, Precoding, Resource Allocation, SWIPT

## I. INTRODUCTION

THE utility of an energy constrained wireless network is often limited due to the reliance on finite energy sources. Owing to its potential to assuage this type of constraint, a technology termed simultaneous wireless information and power transfer (SWIPT) has garnered attention. By combining wireless communication and wireless power transfer concepts, SWIPT uses shared resources to deliver energy and information simultaneously to remote wireless users thereby alleviating the limitations imposed by the energy constraints.

Although radio waves carry both, the transmission of energy and information has generally been studied separately [1], [2]. The study of the simultaneous transmission of these quantities began with [3] and [4], which studied the relationship between data rate and energy transfer. The term SWIPT was first used in [5]. Since then, SWIPT has been the focus of extensive research with works covering a wide variety of topics including, among others, single-carrier systems [6]–[10], multicarrier systems [11]–[18], beamforming [1], [2], [5], [6], [10], [17]–[27], and receiver architecture [1], [2], [5], [7], [24], [25], [28]–[33]. Much of this work is motivated by a desire to increase energy transfer efficiency. Doing so improves the feasibility of SWIPT as the sole energy source for the network and frees energy to be used for increasing the data rate. As such, technologies that improve efficiency, such as orthogonal frequency division multiplexing (OFDM) and beamforming, are of keen interest.

OFDM is a ubiquitous multicarrier technology that enables high data transmission rates [34]–[36] and may be used to realize the advantages of SWIPT through efficient resource allocation methods [15]. One of the earliest papers to study multiuser (MU) multicarrier SWIPT is [11], which examines a multiple-input single-output (MISO) SWIPT network employing orthogonal frequency division multiple access

(OFDMA). OFDMA-based single-input single-output (SISO) MU-SWIPT networks are considered in [12]–[15] and for a SISO-SWIPT relaying network in [16]. Single-user OFDM-based SISO-SWIPT was considered in [15] and for multiple-input multiple-output (MIMO) SWIPT in [17] and [18]. Notably, many OFDM-based MU-SWIPT implementations utilize subcarrier assignment (e.g. OFDMA).

Energy transfer efficiency primarily depends on the signal strength attenuation due to propagation. Multi-antenna beamforming techniques have been applied to improve this aspect of the transfer efficiency as well as enable spatial multiplexing and has become a key SWIPT component [19]. Beamforming for SWIPT was first examined in [5], which studied optimal transmission strategies and the associated information rate and harvested energy tradeoff. Information and energy beamforming designs were investigated for MISO downlinks in [6], [7], [24], MISO interference channels [21], [22], and for MIMO [10], [17], [18], [20], [23], [26], [27], [37], [38]. For an extensive review of the literature on beamforming in wireless networks with energy harvesting, please refer to [19] as well as [1], [2] and the references therein.

The concurrent nature of MU-SWIPT and the added complexity of OFDM and beamforming typically results in challenging non-convex resource allocation problems. The tractability of these problems is often improved by considering simpler systems or making simplifying assumptions. In particular, it is common for OFDM-based SWIPT research to not fully utilize the benefits of multi-antenna beamforming. For example, power allocation for an OFDMA-based MISO-SWIPT system is examined in [11], but the authors treat the beamforming vectors as given and convexify the problem by bounding the impact of interference. This can lead to suboptimal system performance, as is later shown. Other works do not consider beamforming at all [15], [16] or do not support simultaneous multiple access [17], [18]. Those that do utilize multi-antenna beamforming and support multiple users simultaneously often rely on subcarrier assignment [11], [14], [39], which may be redundant since multi-antenna beamforming enables simultaneous multiple access through spatial multiplexing.

Interestingly, both [15] and [16] take a common approach for OFDMA resource allocation and apply it to SWIPT [40]. By utilizing the time-sharing property of multicarrier systems, they argue for the use of Lagrangian duality despite the non-convex nature of the problems they consider. Lagrangian duality decomposes the problem into per-subcarrier sub-problems that can then be more easily solved. In this paper, this idea is applied to SWIPT in a different way. Instead of using the time-sharing property to overcome the non-convexity of subcarrier assignment, time-sharing is utilized to decompose an OFDM-based MU-MISO-SWIPT resource allocation problem to simpler per-subcarrier non-convex problems. This enables the consideration of an OFDM-based system that relies on spatial diversity multiple access (SDMA) through beamforming to support multiple users simultaneously rather than OFDMA, unlike the cited MU-SWIPT works.

Ostensibly, this decomposition allows the use of existing single-carrier solutions for optimal power allocation and beamforming, however some of these algorithms make assumptions that may be suboptimal and many have high computational complexities. In [9], the authors present an algorithm to provide locally optimal transmit covariance matrices for single-carrier MU-MIMO-SWIPT networks, which utilize a strategy based on block-diagonalization to pre-cancel interference at the transmitter. While effective in convexifying the optimization problem, the strategy removes a degree of freedom by canceling the interference. In [10], the authors extended their work by linearizing the interference terms to convexify the problem and then use the majorization-minorization method to iteratively solve it to local optimality. In [6]–[8], the beamforming vectors and power allocation are jointly optimized for single-carrier MU-MISO-SWIPT networks. Through semidefinite relaxation (SDR), the resulting algorithms provide globally optimal solutions, but have significant computational complexity. For example, [7] has complexity that roughly grows with the cubed number of users and the cubed number of transmit antennas. This is later shown to be worse than the proposed method, which grows roughly with the number of energy harvesting users squared and the number of transmit antennas squared. While these solutions optimize the power allocation and beamforming vectors, their high computational complexity make them unsuitable for real-time implementation or for large scale performance simulations. Our proposed algorithm jointly optimizes beamforming vectors and power allocation, but does so at a significantly lower computational complexity than comparable algorithms such as [6]–[8], [10].

There does not appear to be a resource allocation strategy that jointly allocates power and designs beamforming vectors for a MU-MISO broadcast channel (BC) SWIPT system that employs OFDM, but does not resort to using OFDMA. Although there are solutions for the single-carrier problem, they tend to have high computational complexities. As such, a resource allocation algorithm is considered to optimize beamforming vectors and power allocation for a MU-MISO-BC-SWIPT system that employs OFDM without subcarrier assignment. A non-convex optimization problem is formulated in which a weighted sum of user data rates is maximized subject to meeting received power and transmit power constraints. The algorithm exploits the time-sharing property of multicarrier systems to overcome this non-convexity and enables utilizing Lagrangian decomposition to parallelize the problem. Further simplification is achieved via a multiple access channel (MAC) - BC duality, which enables a closed-form solution for the beamforming vectors given the dual MAC power allocation. The dual MAC power allocation is approximated using a successive convex approximation (SCA) technique. The result is an algorithm for the joint optimization of beamforming vectors and power allocation in a MU-MISO-BC-SWIPT system employing OFDM that provides close-to-optimal performance with a lower computational complexity than other existing solutions [6]–[8], [10] and

without resorting to subcarrier assignment.

### ORGANIZATION

The paper is organized as follows. In Section II, the system and signal models are presented. In Section III, the optimization problem is formulated and converted from the BC to the dual MAC through Lagrange duality and a MAC-BC duality. The use of Lagrange duality is justified through the time-sharing property of multicarrier systems, which is defined and described in detail. An algorithm for solving the dual problem along with an exhaustive search algorithm are presented. A method to assess the duality gap called the relative duality gap is also defined. In Section IV, simulations are used to demonstrate the algorithm given various user weights and received power constraints. The performance is then compared to that of an exhaustive search algorithm and another algorithm based on a similar system model [11] to that considered in this paper. The achieved relative duality gap is calculated to further illustrate the near optimality of the solutions provided by the proposed algorithm. Additionally, the computational complexity of the proposed algorithm is compared to single-carrier solutions for similar systems [6]–[8]. Lastly, some conclusions are drawn in Section V.

## II. SYSTEM MODEL

A SWIPT network using OFDM is considered, where the OFDM symbols are comprised of $K$ orthogonal subcarriers. The envisioned network is modeled by a system containing one access point using $N_T$ antennas to deliver data and power to $N$ remote devices (users) each with one antenna, where $N \leq N_T$. The scenario where transmissions are sent from one access point to multiple users is commonly referred to as the BC. It is assumed that there is no inter-carrier interference present, allowing each subcarrier to be modeled independently, and that perfect channel state information is available.

The receiver is an important part of a SWIPT system. A single receiver that can simultaneously decode and harvest energy from the same signal has yet to be developed, so practical schemes utilizing multiple co-located receivers have been utilized instead. Time-splitting (not to be confused with time-sharing) and power-splitting are two such schemes that were first proposed in [5]. In a time-splitting scheme, a receiver either performs information decoding (ID) or energy harvesting (EH). In a power-splitting scheme a power splitter is used to split the incoming signal into two, which are then routed to separate circuits for ID and EH.

In this paper, it is assumed that each remote device utilizes a time-splitting receiver architecture in which the receiver spends $\alpha$ percentage of the time decoding information and $1-\alpha$ harvesting energy. The optimization of the time-splitting ratio is not addressed and will be left for future work.

### BROADCAST CHANNEL

The access point applies a precoder to the symbol vector before transmitting to the remote users, which is modeled on each subcarrier (denoted with subscript $k$) as a BC with

$$\boldsymbol{y}_k = \mathbf{H}_k^{\mathcal{H}} \mathbf{T}_k \boldsymbol{x}_k + \boldsymbol{z}_k. \tag{1}$$

In (1), $\mathbf{H}_k^{\mathcal{H}}$ is the $N \times N_{\mathrm{T}}$ channel matrix, with $[\mathbf{H}_k]_{m,n}^{\mathcal{H}}$ being the transfer function between transmitter $m$ and remote device $n$ (user $n$) evaluated at subcarrier $k$, and $\mathcal{H}$ is the Hermitian transpose operation. Moreover, $\boldsymbol{z}_k$ is an $N \times 1$ vector of additive white Gaussian noise, $\boldsymbol{x}_k$ is the $N \times 1$ vector of transmit symbols for the $N$ users, $\mathbf{T}_k$ is the $N_T \times N$ precoder matrix, and $\boldsymbol{y}_k$ is the $N \times 1$ vector of symbols as received by the $N$ users. Note that matrices are in bold, vectors are italicized and bold, and scalars are italicized.

### PERFORMANCE METRICS

For information transfer, the downstream data rate for user $n$ on subcarrier $k$ may be modeled using:

$$\alpha_n \log_2 \left(1 + \gamma_{k,n}^{\mathrm{BC}}(\mathbf{T}_k, \boldsymbol{s}_k)\right). \tag{2}$$

The total data rate for user $n$ is (2) summed $\forall\ k$. The downstream signal-to-interference-plus-noise ratio (SINR) for user $n$ on subcarrier $k$, $\gamma_{k,n}^{\mathrm{BC}}(\mathbf{T}_k, \boldsymbol{s}_k)$, is a function of the precoder matrix, $\mathbf{T}_k$, and symbol power vector, $\boldsymbol{s_k}$. The symbol power for user $n$, the $n$-th element of $\boldsymbol{s_k}$, is denoted by $s_{k,n}$, and defined as $s_{k,n} \triangleq \mathbb{E}\left[|x_{k,n}|^2\right]$ with $x_{k,n}$ the $n$-th element of $\boldsymbol{x}_k$ and $\mathbb{E}\left[\cdot\right]$ the expected value operator. The factor $\alpha_n \in [0, 1]$ is included in the formulation to reflect the effect of the time-splitting receiver architecture for each user $n$. The SINR is given by:

$$\gamma_{k,n}^{\mathrm{BC}}(\mathbf{T}_k, \boldsymbol{s}_k) = \frac{|\boldsymbol{t}_{k,n}^{\mathcal{H}} \boldsymbol{h}_{k,n}|^2 s_{k,n}}{\sum_{\substack{m=1 \\ m \neq n}}^{N} |\boldsymbol{t}_{k,m}^{\mathcal{H}} \boldsymbol{h}_{k,n}|^2 s_{k,m} + \sigma_{k,n}}, \tag{3}$$

where $\boldsymbol{t}_{k,n}$ is the precoder vector for user $n$, i.e. the $n$-th column of $\mathbf{T}_k$, and $\boldsymbol{h}_{k,n}$ is the transfer function for user $n$, i.e. the $n$-th column of $\mathbf{H}_k$. The additive white Gaussian noise power spectral density experienced by user $n$ and subcarrier $k$ is given by $\sigma_{k,n}$.

It has been observed that the energy harvesting operation is non-linear [1], [2], [32] due to the saturation effect at the capacitor and diode elements of the rectifying circuitry. This effect may be mitigated however, by placing several energy harvesting circuits in parallel yielding an enlarged linear power conversion region in practice [25], [33]. Due to the potential for a sufficiently large linear conversion region, this paper will focus on deriving a resource allocation algorithm without addressing the impact of the energy harvesting circuit non-linearity. The power received by user $n$ on subcarrier $k$ is therefore modeled with:

$$P_{k,n}(\mathbf{T}_k, \boldsymbol{s}_k) = \sum_{m=1}^{N} |\boldsymbol{t}_{k,m}^{\mathcal{H}} \boldsymbol{h}_{k,n}|^2 s_{k,m}. \tag{4}$$

Taking into account the time-splitting parameter, the total received power for user $n$ is $(1-\alpha_n) P_{k,n}(\mathbf{T}_k, \boldsymbol{s}_k)$ summed $\forall\ k$.

## III. OPTIMAL RESOURCE ALLOCATION

### PRIMAL PROBLEM

The resource allocation problem is formulated as the maximization of a weighted sum of data rates over all users and subcarriers, where the total transmit power is constrained to $P_{Total}$ and the minimum per-user received power is constrained to $C_n \; \forall \; n$. The problem is given as

$$\begin{aligned} \underset{\{\mathbf{T}_k, \boldsymbol{s}_k\}\forall k}{\text{maximize}} \; & \sum_{k=1}^{K}\sum_{n=1}^{N} \omega_n \alpha_n \log_2\left(1+\gamma_{k,n}^{\mathrm{BC}}(\mathbf{T}_k, \boldsymbol{s}_k)\right) \\ \text{subject to} \; & \sum_{k=1}^{K}\sum_{n=1}^{N} s_{k,n}||\boldsymbol{t}_{k,n}||_2^2 \leq P_{\mathrm{Total}} \\ & \sum_{k=1}^{K}(1-\alpha_n)P_{k,n}(\mathbf{T}_k, \boldsymbol{s}_k) \geq C_n \; \forall \; n. \end{aligned} \tag{5}$$

The optimal point is chosen by selecting a precoder matrix ($\mathbf{T}_k \; \forall \; k$) and symbol power vector ($\boldsymbol{s}_k \; \forall \; k$) which maximizes the weighted sum. The weights $\omega_n$ are used to weight the importance of individual user data rates as determined by the use-case. Note that the energy harvesting efficiency may be accounted for through the choice of $C_n$.

### LAGRANGE DUAL PROBLEM

The dual problem is formulated by dualizing the constraints and combining them with the objective function in (5). Dualizing the power constraint makes the problem separable over the $K$ subcarriers. Lagrangian decomposition then allows one to evaluate the maximization on a per-subcarrier basis.

The Lagrange dual function is defined as

$$q(\boldsymbol{\lambda}) \triangleq \max_{\mathbf{T},\mathbf{s}} \mathcal{L}(\mathbf{s}, \mathbf{T}, \boldsymbol{\lambda}) \tag{6}$$

where $\boldsymbol{\lambda} = [\lambda_0, ..., \lambda_N]^T$, the Lagrangian, $\mathcal{L}(\mathbf{s}, \mathbf{T}, \boldsymbol{\lambda})$, may be expressed as

$$\mathcal{L}(\mathbf{s}, \mathbf{T}, \boldsymbol{\lambda}) \triangleq \lambda_0 P_{\mathrm{Total}} - \sum_{n=1}^{N} \lambda_n C_n + \sum_{k=1}^{K} \mathcal{L}_k(\mathbf{s}_k, \mathbf{T}_k, \boldsymbol{\lambda}), \tag{7}$$

and $\mathcal{L}_k(\mathbf{s}_k, \mathbf{T}_k, \boldsymbol{\lambda})$ is given as

$$\begin{aligned} \mathcal{L}_k(\mathbf{s}_k, \mathbf{T}_k, \boldsymbol{\lambda}) = & \sum_{n=1}^{N} \omega_n \alpha_n \log_2(1+\gamma_{k,n}^{\mathrm{BC}}(\mathbf{T_k}, \boldsymbol{s}_k)) - \\ & \sum_{n=1}^{N} \boldsymbol{t}_{k,n}^{\mathcal{H}} \Upsilon_k(\boldsymbol{\lambda}) \boldsymbol{t}_{k,n} s_{k,n}. \end{aligned} \tag{8}$$

As noted, the dual function can be simplified to a per-subcarrier maximization of $\mathcal{L}_k$ over the $K$ subcarriers. In addition $\Upsilon_k(\boldsymbol{\lambda})$ is defined as:

$$\Upsilon_k(\boldsymbol{\lambda}) \triangleq \left(\lambda_0 I - \sum_{m=1}^{N} \lambda_m (1-\alpha_m) \boldsymbol{h}_{k,m} \boldsymbol{h}_{k,m}^{\mathcal{H}}\right). \tag{9}$$

If $\Upsilon_k(\boldsymbol{\lambda})$ is not positive definite for all $k$ then the corresponding $\boldsymbol{\lambda}$ cannot be dual optimal because (8) will be unbounded and $q(\boldsymbol{\lambda})$ becomes $+\infty$. The Lagrange dual problem is then given by

$$\begin{aligned} \underset{\boldsymbol{\lambda}}{\text{minimize}} \quad & q(\boldsymbol{\lambda}) \\ \text{subject to} \quad & \boldsymbol{\lambda} \geq 0 \\ & \Upsilon_k(\boldsymbol{\lambda}) \succ 0 \; \forall \; k, \end{aligned} \tag{10}$$

where $\succ \; 0$ denotes that $\Upsilon_k(\boldsymbol{\lambda})$ is required to be positive definite.

### CONVEXITY AND TIME-SHARING

The primal problem in (5) is not convex, so the duality gap may be non-zero. A non-zero duality gap implies that a dual problem (10) solution does not necessarily produce an optimal solution for the primal problem. However, in using data rate as a performance metric subject to transmit and received power constraints, the problem can be cast as a convex optimization problem through time-sharing, where time-sharing can be interpreted as scheduling with variable time slot lengths [41]. Additionally, it has been shown that time-sharing can be approximated in multicarrier systems by assigning different achievable rates to individual subcarriers. This is referred to as the time-sharing property of multicarrier systems.

In maximizing the data rate of a multicarrier system subject to system resource constraints, [42] demonstrated that the time-sharing property enables a zero duality gap for non-convex formulations as long as the time-sharing condition is met. Defined in Definition 1, the time-sharing condition implies that the optimal value of the objective is a concave function of the constraint.

**Definition 1** (Time-sharing Condition [42])**.** Consider an optimization problem of the general form (11) where $\boldsymbol{a}_k$ is a vector of optimization variables, $f_k(\cdot)$ is a scalar function that is not necessarily concave, $\boldsymbol{g}_k(\cdot)$ is a vector valued function that is not necessarily convex, $\boldsymbol{P}$ is a vector of constraints. Here the "$\leq$" is used as a component-wise inequality. Let $\boldsymbol{a}_k^*$ and $\boldsymbol{b}_k^*$ be optimal solutions to (11) with $\boldsymbol{P} = \boldsymbol{P}_a$ and $\boldsymbol{P} = \boldsymbol{P}_b$, respectively. An optimization problem of this form satisfies the time-sharing condition if and only if for any $\boldsymbol{P}_a$ and $\boldsymbol{P}_b$ and for any $0 \leq \nu \leq 1$, there always exists a feasible solution $\boldsymbol{c}_k$ such that $\sum_k^K \boldsymbol{g}_k(\boldsymbol{c}_k) \leq \nu \boldsymbol{P}_a + (1-\nu)\boldsymbol{P}_b$ and $\sum_k^K f_k(\boldsymbol{c}_k) \geq \nu \sum_k^K f_k(\boldsymbol{a}_k^*) + (1-\nu)\sum_k^K f_k(\boldsymbol{b}_k^*)$.

$$\begin{aligned} \text{maximize} & \sum_{k}^{K} f_k(\boldsymbol{a}_k) \\ \text{subject to} & \sum_{k}^{K} \boldsymbol{g}_k(\boldsymbol{a}_k) \leq \boldsymbol{P} \end{aligned} \tag{11}$$

It can be shown that (5) satisfies the time-sharing condition defined in Definition 1 using Theorem 2 in [42]. An intuitive argument provided through Theorem 2 in [42] and rigorously proven in [43], shows that a resource allocation problem using a continuous formulation for the power spectral density over a flat-fading or frequency-selective channel satisfies the time-sharing condition and yields a zero duality gap. It also shows

that the duality gap is zero for the discrete formulation in the limit as $K \to \infty$ and the width of the subcarrier becomes infinitesimal. The results of Theorem 2 in [42] are summarized in Theorem 1. Proposition 1 proves that (5) meets the time-sharing condition in the limit as $K \to \infty$.

**Theorem 1** (Theorem 2 in [42])**.** *A transmit spectrum optimization problem that maximizes a weighted sum of user rates subject to meeting user power constraints always satisfies the time-sharing condition if the channel gains, noise power spectral density, and the interference power spectral density are either constant or continuous functions of frequency. A discrete formulation of the optimization problem also satisfies the time-sharing condition in the limit as the number of subcarriers $K \to \infty$ for a given bandwidth.*

**Proposition 1.** *Equation* (5) *satisfies the time-sharing condition in the limit as $K \to \infty$ for a given bandwidth such that a feasible solution $\boldsymbol{c}_k \; \forall \; k$, associated with power constraints $\boldsymbol{P}_c$ and achievable rate $R_c$, can always be constructed from known optimal solutions.*

*Proof*: Let $\boldsymbol{a}_k^*$ be an optimal solution to (5) for all users associated with an $N+1 \times 1$ vector of power constraints $\boldsymbol{P}_a$, achievable rate $R_a^*$, and is comprised of the optimal beamforming vectors and symbol powers such that $\boldsymbol{a}_k^* = \{\mathbf{T}_k^*, \boldsymbol{s}_k^*\}$ $\forall \; k$. Let $\boldsymbol{b}_k^* = \{\mathbf{T}_k^*, \boldsymbol{s}_k^*\} \; \forall \; k$ be another optimal solution to (5) associated with an $N+1 \times 1$ vector of power constraints $\boldsymbol{P}_b$ and achievable rate $R_b^*$.

1) Equation (5) can be put in the same form as (11) where $\sum_k^K f_k(\boldsymbol{a}_k)$ is given by the objective of (5), $\boldsymbol{a}_k$ is comprised of the beamforming vectors and symbol powers, and the constraint equations are easily reformulated to be in the same form as $\sum_k^K \boldsymbol{g}_k(\boldsymbol{a}_k) \leq \boldsymbol{P}$.
2) $\boldsymbol{c}_k$ can be constructed by interleaving $\boldsymbol{a}_k^*$ and $\boldsymbol{b}_k^*$ with $\nu$ proportionality for any $0 \leq \nu \leq 1$, where $\nu$ proportion of $K$ subcarriers is $\boldsymbol{c}_k = \boldsymbol{a}_k^*$ and $1-\nu$ proportion of $K$ subcarriers is $\boldsymbol{c}_k = \boldsymbol{b}_k^*$.
3) The achieved rate for $\boldsymbol{c}_k$ is approximately equal to the linear combination of the rates given by

$$R_c \approx \nu R_a^* + (1-\nu) R_b^*. \tag{12}$$

4) The power constraint is approximately equal to the linear combination of the constraints given by

$$\boldsymbol{P}_c \approx \nu \boldsymbol{P}_a + (1-\nu) \boldsymbol{P}_b. \tag{13}$$

5) As $K \to \infty$, each subcarrier becomes infinitesimal. By continuity, the channel gains and noise spectra approach a constant value as the width of the subcarrier becomes finer.
6) In the limit as $K \to \infty$, the channel gains and noise spectra become constant over each subcarrier. At which point, the constant channel results from Theorem 1 apply and the approximations in (12) and (13) become equalities given by

$$R_c = \nu R_a^* + (1-\nu) R_b^* \tag{14}$$

and

$$\boldsymbol{P}_c = \nu \boldsymbol{P}_a + (1-\nu) \boldsymbol{P}_b. \tag{15}$$

7) Equations (14) and (15) meet the requirements for the feasible point defined in Definition 1, such that

$$R_c \geq \nu R_a^* + (1-\nu) R_b^* \tag{16}$$

and

$$\boldsymbol{P}_c \leq \nu \boldsymbol{P}_a + (1-\nu) \boldsymbol{P}_b. \tag{17}$$

Therefore (5) satisfies the time-sharing condition in the limit as $K \to \infty$. □

The number of subcarriers is less than infinite in practical systems, so the time-sharing condition is not strictly met and the duality gap may be non-zero. However, [42] asserts that a practical number of subcarriers yields a *near-zero* duality gap, where a practical number is the number of subcarriers chosen such that adjacent subcarriers experience similar fading characteristics that is nearly flat across the subcarrier. This is a common design requirement in multicarrier systems [42]. As such, a network using a practical number of subcarriers is capable of achieving a near optimal solution.

As an example, the work in [44] utilizes the time-sharing property for optimal OFDMA resource allocation. The authors provide an upper-bound on the relative duality gap, which is used to assess how far the resource allocation is from the optimal value. Let $d^* > 0$ and $p^* > 0$ be the optimal values for the dual problem and primal problem, respectively, and let $\hat{p} > 0$ be the feasible primal value. The relative duality gap is then upper-bounded with

$$0 \leq \frac{d^* - p^*}{p^*} \leq \frac{d^* - \hat{p}}{\hat{p}}. \tag{18}$$

The left inequality follows from the positivity of the optimal primal value and weak duality. The right inequality is because a feasible primal value is less than or equal to the optimal primal value, $\hat{p} \leq p^*$. By calculating the bound for the algorithm presented in [44], the authors show that it achieves a relative duality gap of less than $10^{-5}$ for a network with a number of subcarriers as small as 64, which is, as [45] notes, acceptable in practice. Futhermore, the relative duality gap improves with an increasing number of subcarriers. In [46], the rate of decay of the duality gap as a function of the number of subcarriers is shown to be on the order of $K^{-\frac{1}{2}}$ for frequency-selective fading and $K^{-1}$ for flat-fading.

Since finding the globally optimal solution is computationally prohibitive for non-trivial systems, the most that can be hoped for is a computationally efficient method that determines an approximately optimal solution [43]. Several works [15], [16], [44]–[46] have shown that the time-sharing property of multicarrier systems enables such a method through Lagrange duality. However, none of these works consider MU-SWIPT with beamforming and without the use of subcarrier assignment, making the application of time-sharing to the problem considered by this paper novel and thus additionally motivates the approach taken herein.

### MAC-BC DUALITY

MAC-BC duality allows the construction of a MAC problem that has a solution [47] linked to the solution of the BC maximization problem ($\forall\ k$) in (6). The duality asserts that provided $\Upsilon_k(\boldsymbol{\lambda}) \succ 0$, then for any precoder $\mathbf{T}_k$ and positive signal power vector $\boldsymbol{s}_k$ in the BC there exists a dual MAC symbol power vector $\boldsymbol{\delta}_k$ that achieves the same SINR in the MAC (upstream channel $\mathbf{H}_k$ with equalizer $\mathbf{T}_k^{\mathcal{H}}$) as in the BC (downstream channel $\mathbf{H}_k^{\mathcal{H}}$ with precoder $\mathbf{T}_k$) and vice versa. Here the BC problem will be converted to a MAC problem, which is solved to obtain the optimal dual MAC symbol powers and equalizer, which are then converted back to attain the optimal BC symbol powers and precoder.

Applying the duality begins with equating the SINRs

$$\gamma_{k,n}^{\mathrm{BC}}(\mathbf{T}_k, \boldsymbol{s}_k) = \gamma_{k,n}^{\mathrm{MAC}}(\mathbf{T}_k, \boldsymbol{\delta}_k)\ \forall\ k \text{ and } n, \tag{19}$$

where $\gamma_{k,n}^{\mathrm{BC}}(\mathbf{T}_k, \boldsymbol{s}_k)$ is defined in (3) and the dual MAC SINR is defined as

$$\gamma_{k,n}^{\mathrm{MAC}}(\mathbf{T}_k, \boldsymbol{\delta}_k) = \frac{|\boldsymbol{t}_{k,n}^{\mathcal{H}}\boldsymbol{h}_{k,n}|^2\delta_{k,n}}{\sum_{\substack{m=1\\m\neq n}}^{N}|\boldsymbol{t}_{k,n}^{\mathcal{H}}\boldsymbol{h}_{k,m}|^2\delta_{k,m} + \boldsymbol{t}_{k,n}^{\mathcal{H}}\Upsilon_k(\boldsymbol{\lambda})\boldsymbol{t}_{k,n}}. \tag{20}$$

In (20), $\boldsymbol{\delta}_k$ is the dual MAC symbol power vector and $\Upsilon_k(\boldsymbol{\lambda})$ is seen to act as a noise covariance matrix. Since $\Upsilon_k(\boldsymbol{\lambda}) \succ 0$, (19) may be expressed as:

$$\mathbf{Z}_k\boldsymbol{s}_k = \boldsymbol{\sigma}_k \circ \boldsymbol{\delta}_k\ \forall\ k, \tag{21}$$

where $\circ$ is the Hadamard product, $\boldsymbol{\sigma}_k$ is the vector of user noise power spectral densities for subcarrier $k$, and $\mathbf{Z}_k$ is given by:

$$\begin{aligned}[\mathbf{Z}_k]_{ij} &= \sum_{\substack{n=1\\n\neq j}}^{N}|\boldsymbol{t}_{k,j}^{\mathcal{H}}\boldsymbol{h}_{k,n}|^2\delta_{k,n} + \boldsymbol{t}_{k,j}^{\mathcal{H}}\Upsilon_k(\boldsymbol{\lambda})\boldsymbol{t}_{k,j},\ \text{for } i=j\\ [\mathbf{Z}_k]_{ij} &= -\delta_{k,i}|\boldsymbol{t}_{k,j}^{\mathcal{H}}\boldsymbol{h}_{k,i}|^2,\ \text{for } i\neq j.\end{aligned} \tag{22}$$

Since $\mathbf{Z}_k$ is an M-matrix [48], it is guaranteed that for any $\boldsymbol{\delta}_k \geq 0$, solving (21) will yield an $\boldsymbol{s_k} \geq 0$. Summing the rows of (21) yields:

$$\sum_{n=1}^{N}\boldsymbol{t}_{k,n}^{\mathcal{H}}\Upsilon_k(\boldsymbol{\lambda})\boldsymbol{t}_{k,n}s_{k,n} = \boldsymbol{\sigma}_k^{\mathcal{H}}\boldsymbol{\delta}_k. \tag{23}$$

The maximization problem ($\forall\ k$) in (6) may then be simplified further by redefining the problem in terms of the dual MAC data rate and using (23) to arrive at:

$$\underset{\mathbf{T}_k,\boldsymbol{\delta}_k}{\text{maximize}}\ \sum_{n=1}^{N}\omega_n\alpha_n\log_2(1+\gamma_{k,n}^{\mathrm{MAC}}(\mathbf{T}_k,\boldsymbol{\delta}_k)) - \boldsymbol{\sigma}_k^{\mathcal{H}}\boldsymbol{\delta}_k. \tag{24}$$

### DUAL MAC EQUALIZER OPTIMIZATION

Equation (24) is separable when maximizing over $\mathbf{T}_k$ (given $\boldsymbol{\delta}_k$) since the SINR of user $n$ (given by $\gamma_{k,n}^{\mathrm{MAC}}$) only depends on the receive filter $\boldsymbol{t}_{k,n}$ of user $n$ and $\boldsymbol{\sigma}_k^{\mathcal{H}}\boldsymbol{\delta}_k$ does not. This, along with the monotonicity of $log(1+\cdot)$, allows one to only consider $\gamma_{k,n}^{\mathrm{MAC}}(\mathbf{T}_k,\boldsymbol{\delta}_k)$ in the maximization:

$$\underset{\mathbf{T}_k}{\text{maximize}}\ \gamma_{k,n}^{\mathrm{MAC}}(\mathbf{T}_k,\boldsymbol{\delta}_k). \tag{25}$$

The optimal linear equalizer for a MAC is the linear minimum mean square error (MMSE) equalizer and, given the MAC SINR in (20), is readily shown to be:

$$\boldsymbol{t}_{k,n}^{*} = (\sum_{\substack{m=1\\m\neq n}}^{N}\delta_{k,m}\boldsymbol{h}_{k,m}\boldsymbol{h}_{k,m}^{\mathcal{H}} + \Upsilon_k(\boldsymbol{\lambda}))^{-1}\boldsymbol{h}_{k,n}. \tag{26}$$

The expression in (26) enables the MAC SINR to be expressed as a function of $\boldsymbol{\delta}_k$ only, that is

$$\gamma_{k,n}^{\mathrm{MAC}}(\boldsymbol{\delta}_k) = \delta_{k,n}\boldsymbol{h}_{k,n}^{\mathcal{H}}\Big[\sum_{\substack{m=1\\m\neq n}}^{N}\delta_{k,m}\boldsymbol{h}_{k,m}\boldsymbol{h}_{k,m}^{\mathcal{H}} + \Upsilon_k(\boldsymbol{\lambda})\Big]^{-1}\boldsymbol{h}_{k,n}. \tag{27}$$

In turn, (27) is used to reformulate (24) as

$$\underset{\boldsymbol{\delta}_k}{\text{maximize}}\ \sum_{n=1}^{N}\omega_n\alpha_n\log_2(1+\gamma_{k,n}^{\mathrm{MAC}}(\boldsymbol{\delta}_k)) - \boldsymbol{\sigma}_k^{\mathcal{H}}\boldsymbol{\delta}_k. \tag{28}$$

### DUAL MAC SYMBOL POWER OPTIMIZATION

Successive convex approximation (SCA) is employed to optimize the dual MAC symbol power vector $\boldsymbol{\delta}_k$. Successive approximations of (28) are made by fixing constant the dual MAC symbol power values $\delta_{k,m}$ of all users $m \neq n$ and by approximating the data rates with their first order Taylor expansion for all users $m \neq n$. This leads to the maximization being approximated with:

$$\begin{aligned}&\underset{\delta_{k,n}}{\text{maximize}}\ \omega_n\alpha_n\log_2(1+\delta_{k,n}\bar{q}_{k,n}) - (\bar{\phi}_{k,n}+\sigma_{k,n})\delta_{k,n}\\ &\text{subject to}\ \ \delta_{k,n}\geq 0\end{aligned} \tag{29}$$

where $\bar{q}_{k,n}$ is the interference-plus-noise covariance,

$$\bar{q}_{k,n} = \boldsymbol{h}_{k,n}^{\mathcal{H}}\Big[\sum_{\substack{m=1\\m\neq n}}^{N}\bar{\delta}_{k,m}\boldsymbol{h}_{k,m}\boldsymbol{h}_{k,m}^{\mathcal{H}} + \Upsilon_k(\boldsymbol{\lambda})\Big]^{-1}\boldsymbol{h}_{k,n}, \tag{30}$$

$\bar{\phi}_{k,n}$ is from the first order Taylor series expansion,

$$-\bar{\phi}_{k,n} = \frac{\partial}{\partial\delta_k}\Big[\sum_{\substack{m=1\\m\neq n}}^{N}\omega_m\alpha_m log_2(1+\gamma_{k,m}^{\mathrm{MAC}}(\boldsymbol{\delta}_k))\Big]\Big|_{\boldsymbol{\delta}_k=\bar{\boldsymbol{\delta}}_k}, \tag{31}$$

and $\sigma_{k,n}$ is the noise. Terms that are constant over the maximization were removed from the approximation. Karush-Kuhn-Tucker (KKT) conditions enable calculating the optimal value for $\delta_{k,n}$ via the following equation:

$$\delta_{k,n}^{*} = \Big[0, \frac{\frac{\omega_n\alpha_n}{log(2)}}{\bar{\phi}_{k,n}+\sigma_n} - \frac{1}{\bar{q}_{k,n}}\Big]^{+}, \tag{32}$$

where $[x,...,y]^{+} = \max\{x,...,y\}$.

Problem (28) is non-convex, so the employed SCA can only guarantee convergence to a stationary point. Applicable SCA

algorithms for which convergence results are available include BSUM [49] and SJBR [50]. "Block successive upper-bound minimization" (BSUM) utilizes a sequential updating mode referred to as Gauss-Seidel updating, which only updates a single dual MAC symbol power $\delta_{k,n}$. SJBR refers to Algorithm 1 from [50]. SJBR utilizes a parallel updating mode referred to as Jacobi updating, which updates an entire dual MAC symbol power vector, $\boldsymbol{\delta}_k$, by taking a step in the direction of the solution to (29).

### SOLVING THE DUAL PROBLEM

Notably, the feasible set for the dual problem is open due to the positive definite constraint in (10). While the convexity of (10) allows for the use of standard convex optimization tools, this constraint precludes the use of projection-based descent algorithms since they require a closed feasible set. The ellipsoid algorithm [51]–[53] however, is a standard convex optimization tool capable of circumventing this problem by generating iterates interior to the feasibility set. Iterates that fall outside of the set are corrected using feasibility cuts. As such, the ellipsoid algorithm may be used to find values for the Lagrange multipliers $\boldsymbol{\lambda}$. Once $\boldsymbol{\lambda}$ is selected, the resource allocation solves for the optimal dual MAC symbol power, which is then used to calculate the optimal precoder and symbol power for the BC. This is done iteratively until convergence.

### ELLIPSOID INITIALIZATION

An ellipsoid $\mathcal{E}$ can be described as

$$\mathcal{E} = \{\boldsymbol{z} \mid (\boldsymbol{z}-\boldsymbol{\lambda})^T\mathbf{P}^{-1}(\boldsymbol{z}-\boldsymbol{\lambda}) \leq 1\}, \tag{33}$$

where $\boldsymbol{\lambda}$ is the center of the ellipsoid and $\mathbf{P}$ is a positive semidefinite matrix that gives the size and shape of $\mathcal{E}$. The initial ellipsoid may be defined with $\mathbf{P} = diag(\lambda^2_{\mathrm{UB}_0}, \ldots, \lambda^2_{\mathrm{UB}_N})$, where $\boldsymbol{\lambda}_{\mathrm{UB}} = [\lambda_{\mathrm{UB}_0}, \ldots, \lambda_{\mathrm{UB}_N}]$ is an $N+1 \times 1$ vector of upper-bounds for the optimal $\boldsymbol{\lambda}$, i.e. $\boldsymbol{\lambda}^*$. The center of each successive ellipsoid defines $\boldsymbol{\lambda}$ for each iteration.

### OPTIMAL LAGRANGE MULTIPLIER UPPER-BOUNDS

A range of values for the Lagrange multipliers can be determined through an approach detailed in [41] (p. 43). Since $q(\boldsymbol{\lambda})$ is minimized when $\boldsymbol{\lambda} = \boldsymbol{\lambda}^*$, any other $\boldsymbol{\lambda}$ would result in an equal or larger value for $q(\boldsymbol{\lambda})$:

$$q(\boldsymbol{\lambda}) \geq q(\boldsymbol{\lambda}^*). \tag{34}$$

By choosing a feasible value for $\boldsymbol{\lambda}$ such that the positive definite constraint in (10) is met, this relation can then be reformulated to solve for the $\boldsymbol{\lambda}^*$ upper-bounds. Since the channel gain is expected to be significantly less than 1, a reasonable vector is $\boldsymbol{\lambda} = [1, ..., 1]^T$ and leads to:

$$\begin{aligned} q(\mathbf{1}) - \sum_{k=1}^{K}\sum_{n=1}^{N} \omega_n \alpha_n \log_2\left(1+\gamma^{\mathrm{BC}}_{k,n}(\mathbf{T}_k, \boldsymbol{s}_k)\right) \geq \\ \sum_{k=1}^{K}\sum_{n=1}^{N} \lambda^*_n((1-\alpha_n)P_{k,n}(\mathbf{T}_k, \boldsymbol{s}_k) - C_n) + \\ \sum_{k=1}^{K}\sum_{n=1}^{N} \lambda^*_0(P_{\mathrm{Total}} - s_{k,n}||\boldsymbol{t}_{k,n}||^2_2). \end{aligned} \tag{35}$$

Substituting feasible values $\mathbf{s} = \mathbf{s}^{'}$ and $\mathbf{T} = \mathbf{T}^{'}$ into (35) and rearranging yields an expression for the $\lambda^*_n$ upper-bound:

$$\lambda^*_n \leq \frac{q(1) - \sum_{k=1}^{K}\sum_{n=1}^{N} \omega_n \alpha_n \log_2(1+\gamma^{\mathrm{BC}}_{k,n}(\mathbf{T}^{'}_k, \boldsymbol{s}^{'}_k))}{\sum_{k=1}^{K}(1-\alpha_n)P_{k,n}(\boldsymbol{s}^{'}_k, \mathbf{T}^{'}_k) - C_n}, \tag{36}$$

as well as one for the $\lambda^*_0$ upper-bound:

$$\lambda^*_0 \leq \frac{q(1) - \sum_{k=1}^{K}\sum_{n=1}^{N} \omega_n \alpha_n \log_2(1+\gamma^{\mathrm{BC}}_{k,n}(\mathbf{T}^{'}_k, \boldsymbol{s}^{'}_k))}{P_{Total} - \sum_{k=1}^{K}\sum_{n=1}^{N} s^{'}_{k,n}||\boldsymbol{t}^{'}_{k,n}||^2_2}. \tag{37}$$

Equation (36) assumes that the total power constraint is met tightly, meaning that $P_{\mathrm{Total}} - \sum_k^K \sum_n^N s^{'}_{k,n}||\boldsymbol{t}^{'}_{k,n}||^2_2 = 0$. Similarly, (37) assumes that the received power constraints are met tightly, meaning that $C_n - \sum_k^K (1-\alpha_n)P_{k,n}(s^{'}, T^{'}) = 0 \; \forall \; n$. These assumptions increase the ellipsoid search space by increasing the upper-bounds for $\boldsymbol{\lambda}^*$, but also simplifies the calculation of the upper-bounds by rendering them independent of each other (e.g. $\lambda^*_0$ does not appear in (36) and $\lambda^*_n$ does not appear in (37)).

Feasible $\mathbf{s}^{'}$ and $\mathbf{T}^{'}$ are found first by minimizing the transmit power subject to meeting the primal problem (5) constraints, which can be posed as a semidefinite program:

$$\begin{aligned} \underset{\{\mathbf{Q}^{\mathcal{H}}_k\}\forall k}{\text{minimize}} \quad & \sum_{k=1}^{K} \langle \mathbf{Q}^{\mathcal{H}}_k, \mathbf{I} \rangle \\ \text{subject to} \quad & \mathbf{Q}_k \succcurlyeq 0 \; \forall \; k \\ & (1-\alpha_n)\sum_{k=1}^{K} \langle \mathbf{Q}^{\mathcal{H}}_k, \boldsymbol{h}_{k,n}\boldsymbol{h}^{\mathcal{H}}_{k,n} \rangle \; \geq \; C_n \; \forall \; n, \end{aligned} \tag{38}$$

where

$$\mathbf{Q}_k \triangleq \mathbf{T}_k diag(\boldsymbol{s}_k)\mathbf{T}^{\mathcal{H}}_k \tag{39}$$

and

$$\langle \mathbf{A}, \mathbf{B} \rangle \triangleq tr(\mathbf{A}^{\mathcal{H}}\mathbf{B}) \tag{40}$$

is the Frobenius inner product. $\mathbf{Q}_k \succcurlyeq 0$ denotes that $\mathbf{Q}_k$ is required to be positive semidefinite. The trace operator is denoted with $tr(\cdot)$ and $diag(\cdot)$ returns a diagonal matrix with the non-zero elements given by its argument. Once $\mathbf{Q}_k$ is found for all $k$, it is then scaled such that the total power and received power constraints are met strictly. This ensures that the denominators for (36) and (37) are not zero and a feasible value for the upper-bounds can be calculated. Both $\boldsymbol{s}^{'}_k$ and $\mathbf{T}^{'}_k$ may then be found by factoring the scaled $\mathbf{Q}_k$ for all $k$. The upper-bounds for $\boldsymbol{\lambda}^*$ can then be calculated and used to initialize the ellipsoid algorithm.

### ELLIPSOID CUTS

The ellipsoid algorithm iteratively reshapes the ellipsoid using either a feasibility cut or an objective cut. These cuts can be made larger by using deep-cuts [51] for potentially faster convergence. A feasibility cut is made when a dual constraint (specified in (10)) is violated and is based on the normalized subgradient of the violated constraint. Entries associated with the non-violated constraints are set to zero. It should also be noted that the standard form for the dual problem is a maximization. Since the dual problem (10) is a minimization, the sign on each constraint must be inverted to be used with the ellipsoid algorithm.

The Lagrange multiplier constraint function (with inverted sign) is of the form:

$$-m_n(\boldsymbol{\lambda}) = \left[0, ..., -\lambda_n, ..., 0\right]^T. \tag{41}$$

The subgradient of the Lagrange multiplier constraint function is of the form:

$$-\nabla_{\boldsymbol{\lambda}} m_n(\boldsymbol{\lambda}) = \left[0, ..., -1, ..., 0\right]^T. \tag{42}$$

Letting $\rho_1, ..., \rho_m$ be the eigenvalues of $\sum_n^N \lambda_n(1-\alpha_n)\boldsymbol{h}_{k,n}\boldsymbol{h}_{k,n}^{\mathcal{H}}$, the constraint function associated with $\Upsilon_k(\boldsymbol{\lambda})$ is then equivalent to $\lambda_0$ minus the maximum eigenvalue and is given by

$$f_k(\boldsymbol{\lambda}) = \lambda_0 - [\rho_1, ..., \rho_m]^+. \tag{43}$$

If $\boldsymbol{v}_\rho$ is the normalized eigenvector related to the maximum eigenvalue of $\sum_n^N \lambda_n(1-\alpha_n)\boldsymbol{h}_{k,n}\boldsymbol{h}_{k,n}^{\mathcal{H}}$, then the subgradient [54] of $-f_k(\boldsymbol{\lambda})$ is:

$$-\nabla_{\boldsymbol{\lambda}} f_k(\boldsymbol{\lambda}) = \begin{bmatrix} \frac{-\partial f_k(\boldsymbol{\lambda})}{\partial \lambda_0} \\ \frac{-\partial f_k(\boldsymbol{\lambda})}{\partial \lambda_1} \\ \vdots \\ \frac{-\partial f_k(\boldsymbol{\lambda})}{\partial \lambda_N} \end{bmatrix} = \begin{bmatrix} -1 \\ (1-\alpha_1)||\boldsymbol{h}_{k,1}^{\mathcal{H}}\boldsymbol{v}_\rho||_2^2 \\ \vdots \\ (1-\alpha_N)||\boldsymbol{h}_{k,n}^{\mathcal{H}}\boldsymbol{v}_\rho||_2^2 \end{bmatrix}. \tag{44}$$

An objective cut is made when the dual constraints are met, but the stopping criteria is not. The stopping criteria is described in the next subsection. The objective cut is based on the subgradient of the objective function (6) and is:

$$\nabla_{\boldsymbol{\lambda}}\mathcal{L}(\mathbf{s}, \mathbf{T}, \boldsymbol{\lambda}) = \begin{bmatrix} P_{\text{tot}} - \sum_{k=1}^K \sum_{n=1}^N \boldsymbol{t}_{k,n}^{\mathcal{H}}\boldsymbol{t}_{k,n}s_{k,n} \\ -C_1 + (1-\alpha_1)\sum_{k=1}^K \sum_{n=1}^N |\boldsymbol{t}_{k,n}^{\mathcal{H}}\boldsymbol{h}_{k,1}|^2 s_{k,n} \\ \vdots \\ -C_N + (1-\alpha_N)\sum_{k=1}^K \sum_{n=1}^N |\boldsymbol{t}_{k,n}^{\mathcal{H}}\boldsymbol{h}_{k,n}|^2 s_{k,n} \end{bmatrix} \tag{45}$$

### STOPPING CRITERIA

The ellipsoid algorithm has a simple stopping criterion. If $g_i$ is the subgradient of the objective function, defined in (45), on the $i^{th}$ iteration then, if the constraints are met, the algorithm may stop when

$$\sqrt{g_i^T P_i g_i} \leq \epsilon. \tag{46}$$

This guarantees that the achieved objective value is within $\epsilon$ of the optimal objective value.

### ALGORITHM

The problem is iteratively solved using an algorithm with two loops. An outer loop, detailed in Algorithm 1, determines the Lagrange multipliers. Note that Algorithm 1 uses $\vee$ to denote the logical "or" operation. An inner loop, detailed in Algorithm 2, determines the dual MAC symbol power vector based on the Lagrange multipliers. Once the inner loop converges to the dual MAC symbol power vector, the precoding vectors are calculated, and in turn the primal BC symbol power vector is calculated. The precoding vectors and the primal BC symbol power vector are passed back to the outer loop where the constraints are assessed and the loop either converges or iterates.

**Algorithm 1** Outer Loop: Ellipsoid Algorithm

Set tolerance for the objective value, $\epsilon$.
Set $\boldsymbol{\lambda}_{\text{UB}}$ using (36) and (37).
Initialize the ellipsoid: $\mathbf{P} \leftarrow diag(\boldsymbol{\lambda}_{\text{UB}}^2), \boldsymbol{\lambda} \leftarrow \mathbf{1}$

```
i = 0
while Not Converged do
    i = i + 1
    while λ < 0 ∨ f_k(λ) ≤ 0 do
        Ellipsoid constraint cut with (42) or (44).
    [T, s] = SCA(ω, λ, H, σ)
    if [T, s] is best then
        Save [T, s].
    if sqrt(g_i^T P_i g_i) ≤ ε then
        Converged, return best [T, s].
    else
        Ellipsoid objective cut with (45).
```

**Algorithm 2** Inner Loop: Successive Convex Approximation

```
function SCA(ω,λ,H,σ)
    δ ← 0
    for all k ∈ {1, ..., K} do
        while Not Converged do
            for all n ∈ {1, ..., N} do
                Calculate q_{k,n} using (30).
            for all n ∈ {1, ..., N} do
                Calculate φ_{k,n} using (31).
            δ_old = δ_k
            Calculate δ_k using (32) with BSUM or SJBR.
            step ← |δ_old − δ_k| / (δ_old + δ_k)
            if step < Threshold then
                Converged
        Calculate T_k based on (26).
        s_k ← δ_k using (23).
    return T, s
```

### GLOBALLY OPTIMAL SOLUTION

As noted (28) is non-convex, so achieving the global optimum cannot be guaranteed with the SCA algorithms. An

alternative is to find the global optimum through exhaustive search. Exhaustively searching for the global optimum of the primal problem (5) would require exponential computational complexity in $NK$. However, a strategy detailed in [55] and [56] can be used to reduce the computational complexity to be exponential in $N$ by exhaustively searching for the global optimum to the dual problem. The idea is to iteratively solve for the Lagrange multipliers as detailed in the previous subsections and then for each iteration of $\boldsymbol{\lambda}$ solve the dual problem in (28) for all $k$ through exhaustive search. The global optimum in the BC can then be determined from the global optimum found by this algorithm in the dual MAC.

According to [56], defining the boundaries for the exhaustive search in the dual MAC is not trivial, but a straightforward strategy is to exhaustively search over a grid of dual MAC SINR values. Evaluating the Lagrangian (7) requires finding $\boldsymbol{\delta}_k$ for each dual MAC SINR vector in the set through (27). This $\boldsymbol{\delta}_k$ may be found through a fixed point iteration

$$\delta_{k,n}(i+1) = \frac{\gamma_{k,n}^{\mathrm{MAC}}}{\boldsymbol{h}_{k,n}^{\mathcal{H}} \mathbf{Q}_{k,n}^{-1}(i) \boldsymbol{h}_{k,n}}, \ \forall \ n \tag{47}$$

where

$$\mathbf{Q}_{k,n}(i) = \sum_{\substack{m=1 \\ m \neq n}}^{N} \delta(i)_{k,m} \boldsymbol{h}_{k,m} \boldsymbol{h}_{k,m}^{\mathcal{H}} + \Upsilon_k(\boldsymbol{\lambda}). \tag{48}$$

Algorithm 3 outlines the exhaustive search algorithm, which can simply replace the SCA function in Algorithm 1.

**Algorithm 3** Inner Loop: Exhaustive Search

**function** ES($\boldsymbol{\omega}$,$\boldsymbol{\lambda}$,$\mathbf{H}$,$\boldsymbol{\sigma}$)
  Initialize grid of SINRs
  $\delta \leftarrow 0$
  **for all** $k \in \{1, ..., K\}$ **do**
    **for all** $\boldsymbol{\gamma}_k^{\mathrm{MAC}} \in grid$ **do**
      Iteratively calculate $\boldsymbol{\delta}_k$ using (47).
      Calculate $\mathcal{L}_k(\boldsymbol{\delta}_k)$ using (28), keep best so far.
    Calculate $\mathbf{T}_k$ based on (26).
    $\boldsymbol{s}_k \leftarrow \boldsymbol{\delta}_k$ using (23).
  **return** $\mathbf{T}, \boldsymbol{s}$

## IV. SIMULATIONS

The capability of the algorithm to maximize the network data rate through joint optimization of the beamforming vectors and power allocation is demonstrated in this section through simulation. The simulation examines the impact of the user role (e.g. ID or EH), per-user weight, $\omega_n$, and received power constraints. Comparisons are made between the proposed algorithm and the exhaustive search algorithm as well as other related algorithms. The relative duality gap is also used to illustrate the near-zero duality gap.

### SIMULATION PARAMETERS

The general simulation parameters are described in Table 1. Unless otherwise noted, the network is comprised of three users referred to as user-1, user-2, and user-3, which are divided into two user sets: ID users and EH users. ID users have a time-splitting ratio of $\alpha_n = 1$, while the EH users have a time-splitting ratio of $\alpha_n = 0$. The received power constraint is set as a fraction of the maximum achievable received power for each EH user. The fading environment is modeled as Rayleigh. The MISO channel is modeled using the MATLAB communications toolbox.

**TABLE 1.** Simulation Parameters

| Parameter | Value |
|---|---|
| First Subcarrier Frequency, $f_0$ | 2.4 GHz |
| Number of Subcarriers,$K$ | 1024 |
| Subcarrier Bandwidth | 19531.25 Hz |
| OFDM Bandwidth | 20 MHz |
| Total Power Constraint, $P_{\mathrm{Total}}$ | 30 dBm or 50 dBm |
| Large Scale Pathloss | 30 dB |
| Number of Transmit Antennas, $N_{\mathrm{T}}$ | 6 or 10 |
| Number of Users, $N$ | 3 |
| Information User Set, $\alpha_n = 1$ | user-1 and user-2 |
| Harvesting User Set, $\alpha_n = 0$ | user-3 |
| Fading Environment | Rayleigh [57] |
| Noise Power Density,$\sigma$ | -112 dBm/Hz |

### OPERATIONAL REGIONS

Operational regions are presented in this section to illustrate the relationship between system parameters. First the sum-rate sum-power region for two transmit power constraints $P_{\mathrm{Total}} = \{30, 50\}$ dBm, $K = 1024$, $\omega_n = 1 \ \forall \ n$, and for various user configurations are examined. Second, the rate region as a function of the received the power constraint and user weight $\omega_n$ is illustrated.

#### Sum-Rate Sum-Power Region

The sum-rate sum-power region is used to visualize the relationship between the sum data rate and the sum received power by varying the received power constraints for different network instantiations. Each trace in the sum-rate sum-power region represents a network configuration. The EH user set for a particular trace is denoted in the legend. The remaining nodes belong to the ID user set.

Figure 1 illustrates this relationship for $P_{\mathrm{Total}} = 30$ dBm and shows that the sum-rate sum-power region changes dramatically with the number of EH and ID users as well as the particular users placed in each set. Interestingly, even with the received power constraint set to zero, the EH users still receive some power, implying that it did not improve the sum data rate to completely cancel this interference. Figure 2 illustrates that increasing the transmit power constraint to $P_{\mathrm{Total}} = 50$ dBm increases the size of the rate-power regions. The maximum sum received power is achieved when all users are EH users. Notice that the maximum received power for each network scenario increases linearly with $P_{\mathrm{Total}}$. The maximum sum power - achieved when all users are EH users - increases

from 17.097μW for $P_{\text{Total}} = 30$ dBm to 1.7097mW for $P_{\text{Total}} = 50$ dBm.

The network data rate increases significantly in both figures each time an ID user is added. This is due in part to the system relying on SDMA through beamforming for multiple access, allowing all ID users to simultaneously utilize the entire band. A comparable system that utilizes subcarrier assignment necessarily subdivides the band into mutually exclusive sub-bands that are assigned to particular users. Since data rate increases linearly with bandwidth and logarithmically with signal power, subcarrier assignment results in lower network data rates. The network achieves its maximum data rate when all users are ID users. The maximum achieved sum-rates are 10.8 kbps/Hz and 30.52 kbps/Hz for $P_{\text{Total}} = 30$ dBm and $P_{\text{Total}} = 50$ dBm, respectively.

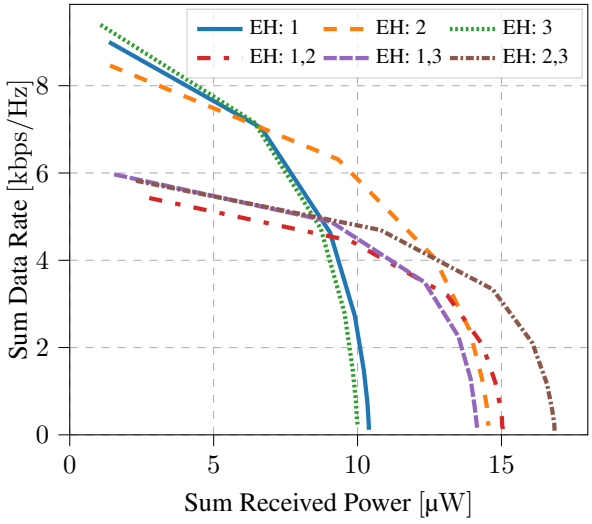


**FIGURE 1.** Sum-rate sum-power curve with $K = 1024$ and $P_{\text{Total}} = 30$ dBm for various user roles. The users that make up the EH user set are denoted in the legend for each curve. The users that are not listed act as ID users.

### Rate Region

The rate region may be visualized by varying the ID user weights for a particular network configuration and received power constraints. Several rate regions were generated as depicted in Figure 3 for the network configuration listed in Table 1 and corresponds to the rate-power trace labeled "EH: 3" in Figure 1. The individual user data rate for each curve varies according to the weights, $\omega_n$, where the peak user-1 data rate corresponds to $\omega_1 = 1$ and $\omega_2 = 0$ and the peak user-2 data rate corresponds to $\omega_1 = 0$ and $\omega_2 = 1$. Since user-3 is never in a decoding mode ($\alpha_3 = 0$), its corresponding weight, $\omega_3$, has no effect on the rate region. However, as the received power constraint increases for user-3 the subsequent rate regions decrease in size. Notably, the reduction in the rate region increases dramatically as the received power constraint approaches the maximum feasible value. In addition, each rate region appears to be a convex set.

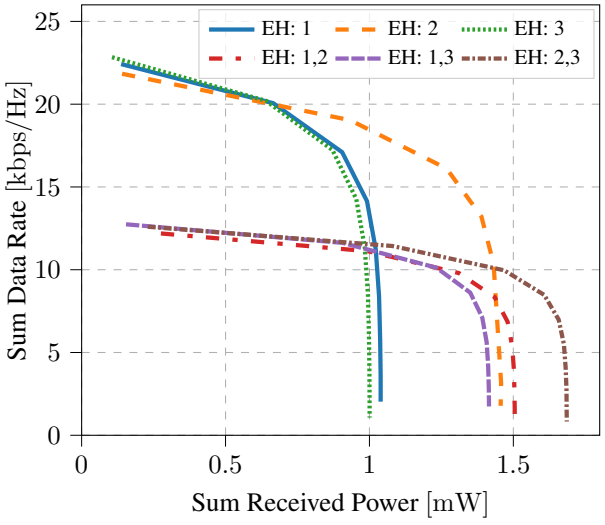


**FIGURE 2.** Sum-rate sum-power curve for various user roles similar to Figure 1, but with $P_{\text{Total}} = 50$ dBm.

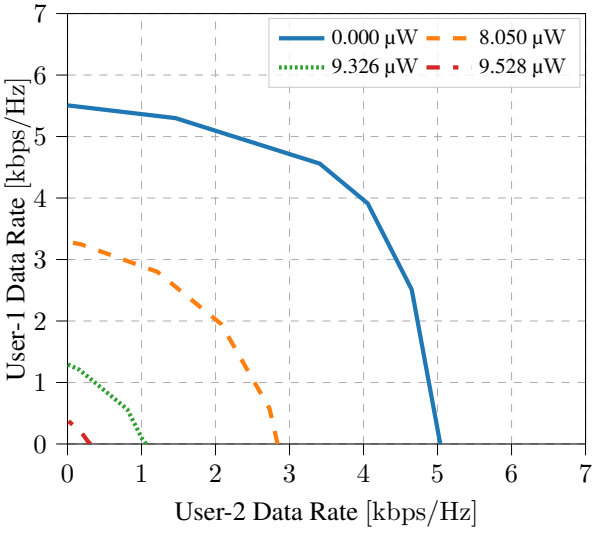


**FIGURE 3.** Network rate region as a function of the user-3 received power constraint and the relative weights for user-1, $\omega_1$, and user-2, $\omega_2$. The transmit power constraint is $P_{\text{Total}} = 30$ dBm. The data rates are summed over all subcarriers.

### *RELATIVE DUALITY GAP*

Equation (18) can be used to assess the impact of the time-sharing property by calculating an upper-bound for the relative duality gap between the solutions for the dual problem (10) and the primal problem (5). Exhaustive search can be used to find the optimal dual value $d^*$. Once $d^*$ is known, $\hat{p}$ can be calculated using the solution to the dual problem and then the upper-bound for the relative duality gap can be calculated.

The relative duality gap is calculated for the network described in Table 1 for $P_{Total} = \{30, 50\}$ dBm and $N_T = \{6, 10\}$ over a range of subcarriers $K = \{16, 32, 64, 128, 256, 512\}$. To do so, sum-rate sum-power curves are generated for each configuration in which one or none of the users are in the EH user set and the remaining

users are in the ID user set. The upper-bound for the relative duality gap is then calculated for each point. All points are then averaged to find the mean value for each number of subcarriers, $K$. Depicted in Figure 4, the results show that the exhaustive search has an average relative duality gap of less than $10^{-3}$ for $K \geq 32$, which decreases monotonically with an increasing number of subcarriers. For $N_T = 6$, $N = 3$, $P_{Total} = 30$ dBm, a relative duality gap of $7 \times 10^{-5}$ is achieved with $K = 512$. This translates into an average sum data rate loss of $0.296$ bps/Hz, which is insignificant compared to the average sum data rate $4275.47$ bps/Hz. This clearly shows that using a reasonable number of subcarriers (e.g. $K \geq 32$) results in a relative duality gap that is small enough for practical purposes. Additionally, it appears that the relative duality gap also improves with a larger transmit power constraint and more transmit antennas.

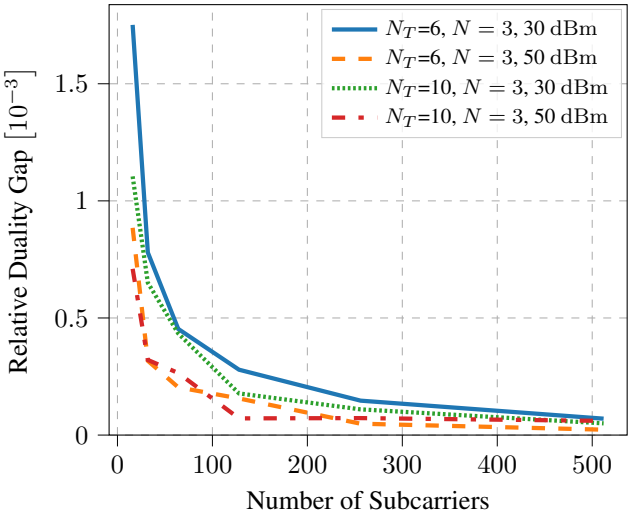


**FIGURE 4.** The mean relative duality gap for the exhaustive search algorithm with $N_T = \{6, 10\}$,$N = 3$, and $P_{Total} = \{30, 50\}$ dBm as a function of the number of subcarriers.

### *ALGORITHM COMPARISON*

The proposed algorithm is compared to two alternative algorithms, i.e. the exhaustive search algorithm and a selected algorithm (P5.1) from [11], referred to as the Huang-Larsson algorithm. The exhaustive search algorithm is Algorithm 1 with the function SCA$(\boldsymbol{\omega}, \boldsymbol{\lambda}, \mathbf{H}, \boldsymbol{\sigma})$ replaced with the function ES$(\boldsymbol{\omega}, \boldsymbol{\lambda}, \mathbf{H}, \boldsymbol{\sigma})$ defined in Algorithm 3. The Huang-Larsson algorithm utilizes a system model (multicarrier MISO-SWIPT with OFDMA) that is similar to the model studied in this paper. For the purpose of comparison, the Huang-Larsson algorithm is extended to solve for this system. A comparison is then made between the rate-power regions of the proposed algorithm, the exhaustive search algorithm, and the Huang-Larsson algorithm.

#### Rate-Power Region: Huang-Larsson Algorithm

The authors in [11] examine a system similar to that presented in this paper, but only optimize the power allocation while assuming the beamforming vectors are given. Linear precoders that may be generated without knowledge of the power allocation include the zero-forcing (ZF) precoder and the maximum ratio transmission (MRT) precoder. Although the ZF precoder is asymptotically optimal for high signal to noise ratios (SNRs) it is not for low SNRs [58]. Conversely, the MRT precoder is near optimal for low SNRs, but not for high SNRs [58]. The MMSE linear precoder combines the asymptotic properties of the ZF and MRT precoders and optimally trades off capturing energy of the data stream and nulling the inter-stream interference to achieve close to optimal performance for both low and high SNRs [48]. However, the MMSE precoder does this by taking into account the distribution of the transmit power and the noise power, which necessitates knowing the power allocation during the design process. Unlike the problem considered in this paper, [11] assumes the precoders are given before determining the power allocation and thus cannot use the MMSE precoder. Not jointly optimizing the power allocation and beamforming vectors therefore leads to a suboptimal solution. To illustrate, the Huang-Larsson algorithm was modified here to optimize over an entire OFDM symbol, without power-splitting, with fixed time-splitting ratios, and in conjunction with a ZF precoder, defined by the normalized pseudo-inverse of the MISO channel, as well as with a MRT precoder defined by the normalized channel transfer function.

The proposed algorithm is expected to perform equivalently or better than the Huang-Larsson algorithm for both the ZF and MRT precoder. The rate-power regions are compared in Figure 5. As expected, the Pareto edge of the Huang-Larsson algorithm for both precoders fall within the rate-power region of the proposed algorithm, indicating that the proposed algorithm achieves a higher data rate for a given received power constraint. It is notable that the proposed algorithm achieves higher data rates even at the extremes, when the received power constraint is 0 µW and when it is 14.56 µW. Clearly, the joint optimization provides the flexibility to design beamforming vectors better suited for simultaneous information and power transfer, allowing the algorithm to achieve higher data rates given the constraints.

#### Rate-Power Region: Exhaustive Search

The exhaustive search algorithm takes a considerable amount of time to run, but this may be reduced by limiting the grid search to more granular bit-loadings. A reasonable restriction is integer bit-loading since the associated constellation size is based on the achievable integer bit-loading. Unfortunately, integer bit-loading limits the attainable received powers to only select points on the rate-power region. This limitation is noticeable at the upper-end of the range of achievable received powers when power is concentrated on fewer subcarriers and the received SINRs correspond to non-integer bit-loading. Achieving these received powers requires an increased grid search resolution.

In generating the sum-rate sum-power region, two separate grid search resolutions are used. A grid search comprised of

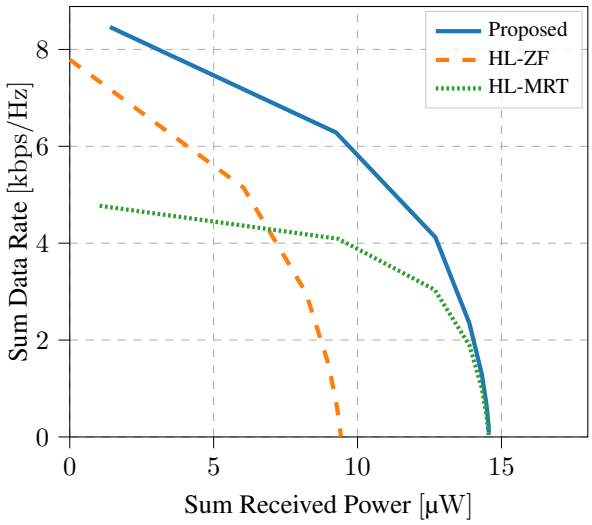


**FIGURE 5.** Sum-rate sum-power region generated by the proposed algorithm, the Huang-Larsson algorithm using a zero-forcing precoder (HL-ZF), and the Huang-Larsson algorithm using a maximum ratio transmission precoder (HL-MRT). The maximum sum received power achieved by HL-ZF is 9.4184 $\mu$W and by HL-MRT is 14.562 $\mu$W.The network configuration is listed in Table 1 and corresponds to the rate-power trace labeled "EH: 2" in Figure 1

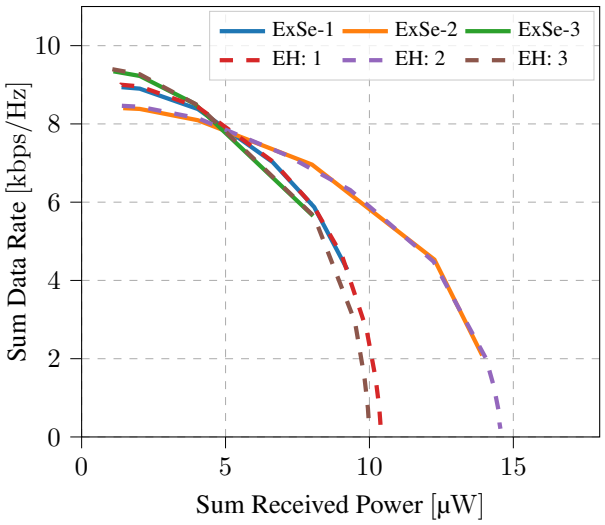


**FIGURE 6.** Sum-rate sum-power region generated by the proposed algorithm and the exhaustive search algorithm using 1024 subcarriers. Traces labeled with an "EH" are the results for the proposed algorithm. Traces labeled with an "ExSe" are for the exhaustive search.

integer bit-loadings is used for received power constraints associated with integer bit-loadings less than or equal to the maximum achievable integer bit-loading. For received power constraints associated with bit-loadings greater than the maximum achievable integer bit-loading, an increased resolution of $0.2$ bps/Hz instead of $1$ bps/Hz is used. For comparison, the proposed algorithm is used to solve for selected points over the full range of feasible received powers. The network configuration is listed in Table 1 with $P_{\text{Total}} = 30$ dBm. The results for both algorithms are illustrated in Figure 6. The traces labeled "EH: 1","EH: 2", and "EH: 3" correspond with the same traces labeled in Figure 1 using the proposed algorithm. The traces labeled "ExSe-1","ExSe-2", and "ExSe-3" correspond to the same traces, respectively, but using the exhaustive search algorithm.

The exhaustive search algorithm generates a near-optimal solution to the primal problem. Figure 6 clearly shows that the proposed algorithm tracks the curve of the exhaustive search algorithm quite closely. This close approximation implies that the proposed algorithm also produces a solution that is a close approximation of the globally optimal solution, but with significantly less computational effort.

### *ASYMPTOTIC COMPUTATIONAL COMPLEXITY*

The outer-loop of the proposed algorithm uses the ellipsoid algorithm to solve for the Lagrange multipliers. Although this algorithm converges in polynomial time, it is still slower than other algorithms and improvements can be readily made. As such, the contribution of the outer loop to the total complexity will be abstractly referred to as $I_o$ per iteration. In turn, the inner-loop calculates the dual MAC symbol power vector and is dominated by a single matrix inversion for $N_E < N_T$ with computational complexity $\mathcal{O}(N_T^3)$ per inner-loop iteration, where $N_E$ is the number of harvesting users with nonzero received power constraints. This can be reduced through rank-1 updates to $\mathcal{O}(N_T^2)$, which then makes the formation of the matrix itself the dominating operation with an asymptotic computational complexity of $\mathcal{O}(N_T N_E^2 + N_T^2 N_E + N_T^2)$. Due to Lagrangian decomposition, the computational complexity grows linearly with the number of subcarriers $K$ per iteration. Including the outer-loop complexity and the linear relationship to the number of subcarriers, the asymptotic computational complexity is found to be $\mathcal{O}(I_o K(N_T N_E^2 + N_T^2 N_E + N_T^2))$.

As noted, the time-sharing property also enables using exhaustive search or other existing single-carrier algorithms for the inner-loop instead of the proposed MAC-BC duality based algorithm. Ignoring the contribution of the outer-loop, $I_o$, the inner-loop computational complexities may be compared to assess how well the algorithms scale with the network size. An inner-loop that utilizes the exhaustive search algorithm has a computational complexity of $\mathcal{O}(K|\mathcal{B}|^N)$, where $|\mathcal{B}|$ is the cardinality of the search grid. Since the complexity is exponential in $N$, exhaustive search clearly has a much higher asymptotic computational complexity than the proposed algorithm. Similar to this paper, MU-MISO-SWIPT networks are considered in [6]–[8] for single-carrier systems. An inner-loop utilizing the algorithm in [7] has a computational complexity of $\mathcal{O}(K\sqrt{NN_T}(N^3N_T^2 + N^2N_T^3))$. Computational complexities were not given for [6] and [8]. However, they do consider SDR-based optimal beamforming routines and [6] notes that it was shown in [59] that SDRs for optimal beamforming problems can be solved with a worst-case complexity of $\mathcal{O}(K(N_I^3N_T^{3.5} + N_I^4)log(\frac{1}{\epsilon}))$, where $\epsilon$ is the solution tolerance and $N_I$ is the number of ID users.

Since $N_T$ is lower-bounded by $N$ for all of the considered algorithms, the worst-case complexity occurs when $N_T = N$

and the best-case occurs when $N = 1$. In comparing the worst-case complexities, it is found the proposed algorithm grows at a slower rate by roughly a factor of $N_T^3$. In particular, when $N_T = N_E$, the complexity for the proposed algorithm is $\mathcal{O}(K(2N_T^3 + N_T^2))$. When $N_T = N_I = N$, the complexity for [7] is $\mathcal{O}(K2N_T^6)$ and for both [6], [8] is $\mathcal{O}(K(N_T^{6.5} + N_T^4)log(\frac{1}{\epsilon}))$. In comparing the best-case complexities for [6]–[8] to the worst-case of the proposed algorithm, it is found that the computational complexity for the proposed algorithm still grows at a slower rate, but by roughly a factor of $\sqrt{N_T}$. Specifically, when $N = N_I = 1$, the complexity for [7] is $\mathcal{O}(K\sqrt{N_T}(N_T^3 + N_T^2))$ and for both [6], [8] is $\mathcal{O}(K(N_T^{3.5} + 1)log(\frac{1}{\epsilon}))$. Lastly, if the best-case is considered for the proposed algorithm, the complexity improves to $\mathcal{O}(K(2N_T^2 + N_T))$ when $N_E = 1$. If there are no EH users ($N_E = 0$) it improves further to $\mathcal{O}(KN_T^2)$. It is therefore clear that the single-carrier solutions can have significantly greater computational complexity and the proposed method is thus better suited for larger more pragmatic multicarrier systems.

### *SUMMARY*

The functionality of the proposed algorithm has been demonstrated through simulation. First, the tradeoff between network data rates and receive power as a function network configuration was illustrated, showing that as the sum received power constraint increased the sum data rate decreased. It was observed that this relationship depended heavily on which users were energy harvesters and which were information decoders. Next, simulations showed the impact of individual user data rate weighting and the received power constraint; depicting that the rate region decreases in size as the receive power requirements increase and that individual user data rate is a function of the relative user weightings. Lastly, it has been shown that given a feasible received power constraint, the proposed algorithm outperforms the Huang-Larsson algorithm in terms of data rates achieved. This is because Huang-Larsson only optimized the power allocation while assuming the beamforming vectors are given while the proposed algorithm jointly optimized both the power allocation and beamforming vectors.

Ostensibly, the time-sharing property may be utilized to enable applying existing single-carrier solutions to the multicarrier system considered. However, the relevant solutions have higher computational complexities. To illustrate, the asymptotic computational complexity for the proposed algorithm was analyzed and compared to existing single-carrier solutions for MU-MISO-SWIPT networks. It was shown that the computational complexity of the proposed algorithm grows at a slower rate with an increasing network size and therefore better lends itself to solving resource allocation problems for larger multicarrier systems.

Due to the non-convexity of the problem considered, it is important to justify the methods used by illustrating that the resulting resource allocation is close to optimal. It was first demonstrated that the relative duality gap is small, less than $10^{-3}$, for a practical number of subcarriers and decreases monotonically as the number of subcarriers increase. This result justifies utilizing Lagrangian decomposition despite the non-convexity of the primal problem since the gap is small enough for practical purposes. Next, the results from the proposed algorithm was shown to be close to the results from an exhaustive search algorithm, thereby implying that the results are near-optimal.

## V. CONCLUSION

This paper presents a resource allocation algorithm that jointly optimizes power allocation and beamforming vectors for a MU-MISO-BC-SWIPT network employing OFDM. Existing solutions for multicarrier systems rely on subcarrier assignment such as OFDMA for multiple access, which limits the degree of freedom and the achievable data rate. The presented algorithm expands on these solutions by relying on SDMA through beamforming for multiple access instead of subcarrier assignment thereby making it a novel and more flexible solution. Existing single-carrier solutions may be used in conjunction with the time-sharing property to solve for multicarrier systems, but at a cost of higher asymptotic computational complexity than the proposed algorithm.

The capability of the algorithm to optimize the system given the weights, constraints, and propagation environment has been demonstrated in Section IV. Simulations demonstrate that the algorithm works as expected with the rate region decreasing in size as the received power requirements increase and that individual user data rate is a function of the relative user weights. Given a feasible received power constraint, the proposed algorithm outperforms the Huang-Larsson algorithm [11] for a multicarrier system and performs similarly to an exhaustive search algorithm in terms of the achieved data rates. The proposed algorithm has also been shown to have a significantly smaller computational complexity than the exhaustive search algorithm and comparable single-carrier systems [6]–[8], indicating that it better lends itself for solving resource allocation problems for larger more pragmatic multicarrier systems. Lastly, despite the non-convexity of the considered problem, it has been demonstrated that the relative duality gap is small and the algorithm is able to achieve near-optimal results.

In conclusion, the algorithm is a computationally efficient method that determines an approximately optimal solution. It is a flexible and scalable means to allocate resources according to end-user defined data rate weights, received power conditions, and user roles. Future directions of work may consider optimizing over the time-splitting ratio, power-splitting ratio, or investigate the effect of non-linear power harvesting. Additionally, it appears that this work can be readily extended to MU-MIMO-BC-SWIPT networks.

## ACKNOWLEDGMENT

All algorithms were written in MATLAB. CVX [60], [61] was used to solve (38) and a modified form of (P5.1) from [11].

## REFERENCES

[1] Y. Zeng, B. Clerckx, and R. Zhang, "Communications and Signals Design for Wireless Power Transmission," *IEEE Trans. Commun.*, vol. 65, no. 5, pp. 2264–2290, May 2017.
[2] B. Clerckx, R. Zhang, R. Schober, D. W. K. Ng, D. I. Kim, and H. V. Poor, "Fundamentals of Wireless Information and Power Transfer: From RF Energy Harvester Models to Signal and System Designs," *IEEE J. Sel. Areas Commun.*, vol. 37, no. 1, pp. 4–33, Jan. 2019.
[3] L. R. Varshney, "Transporting information and energy simultaneously," in *2008 IEEE International Symposium on Information Theory*, Jul. 2008, pp. 1612–1616.
[4] P. Grover and A. Sahai, "Shannon meets Tesla: Wireless information and power transfer," in *2010 IEEE International Symposium on Information Theory*, Jun. 2010, pp. 2363–2367.
[5] R. Zhang and C. K. Ho, "MIMO Broadcasting for Simultaneous Wireless Information and Power Transfer," *IEEE Trans. Wirel. Commun.*, vol. 12, no. 5, pp. 1989–2001, May 2013.
[6] J. Xu, L. Liu, and R. Zhang, "Multiuser MISO Beamforming for Simultaneous Wireless Information and Power Transfer," *IEEE Trans. Signal Process.*, vol. 62, no. 18, pp. 4798–4810, Sep. 2014.
[7] Q. Shi, L. Liu, W. Xu, and R. Zhang, "Joint Transmit Beamforming and Receive Power Splitting for MISO SWIPT Systems," *IEEE Trans. Wirel. Commun.*, vol. 13, no. 6, pp. 3269–3280, Jun. 2014.
[8] Z. Zhu, Z. Wang, X. Gui, and X. Gao, "Robust downlink beamforming and power splitting design in multiuser MISO SWIPT system," in *2014 IEEE/CIC International Conference on Communications in China (ICCC)*, Oct. 2014, pp. 271–275.
[9] J. Rubio, A. Pascual-Iserte, D. P. Palomar, and A. Goldsmith, "SWIPT techniques for multiuser MIMO broadcast systems," in *2016 IEEE 27th Annual International Symposium on Personal, Indoor, and Mobile Radio Communications (PIMRC)*, Sep. 2016, pp. 1–6.
[10] ——, "Joint Optimization of Power and Data Transfer in Multiuser MIMO Systems," *IEEE Trans. Signal Process.*, vol. 65, no. 1, pp. 212–227, Jan. 2017.
[11] K. Huang and E. Larsson, "Simultaneous Information and Power Transfer for Broadband Wireless Systems," *IEEE Trans. Signal Process.*, vol. 61, no. 23, pp. 5972–5986, Dec. 2013.
[12] X. Zhou, R. Zhang, and C. K. Ho, "Wireless Information and Power Transfer in Multiuser OFDM Systems," *IEEE Trans. Wirel. Commun.*, vol. 13, no. 4, pp. 2282–2294, Apr. 2014.
[13] Z. B. Zawawi, J. Park, and B. Clerckx, "Simultaneous Wireless Information and Power Transfer in a two-user OFDM Interference Channel," in *2015 International Symposium on Wireless Communication Systems (ISWCS)*, Aug. 2015, pp. 266–270.
[14] S. Yin and Z. Qu, "Resource Allocation in Multiuser OFDM Systems With Wireless Information and Power Transfer," *IEEE Commun. Lett.*, vol. 20, no. 3, pp. 594–597, Mar. 2016.
[15] W. Lu, Y. Gong, J. Wu, H. Peng, and J. Hua, "Simultaneous Wireless Information and Power Transfer Based on Joint Subcarrier and Power Allocation in OFDM Systems," *IEEE Access*, vol. 5, pp. 2763–2770, 2017.
[16] Y. Liu and X. Wang, "Information and Energy Cooperation in OFDM Relaying: Protocols and Optimization," *IEEE Trans. Veh. Technol.*, vol. 65, no. 7, pp. 5088–5098, Jul. 2016.
[17] X. Peng, P. Wu, and M. Xia, "MSE-Based Transceiver Optimization for Multicarrier MIMO SWIPT Systems," in *2020 IEEE Wireless Communications and Networking Conference (WCNC)*, May 2020, pp. 1–6.
[18] ——, "Optimization for Multicarrier MIMO SWIPT Systems Under MSE QoS Constraint," in *2020 IEEE 91st Vehicular Technology Conference (VTC2020-Spring)*, May 2020, pp. 1–5.
[19] X. Lu, P. Wang, D. Niyato, D. I. Kim, and Z. Han, "Wireless Networks With RF Energy Harvesting: A Contemporary Survey," *IEEE Commun. Surv. Tutor.*, vol. 17, no. 2, pp. 757–789, Secondquarter 2015.
[20] C. Song, C. Ling, J. Park, and B. Clerckx, "MIMO broadcasting for simultaneous wireless information and power transfer: Weighted MMSE approaches," in *2014 IEEE Globecom Workshops (GC Wkshps)*, Dec. 2014, pp. 1151–1156.
[21] S. Timotheou, I. Krikidis, G. Zheng, and B. Ottersten, "Beamforming for MISO Interference Channels with QoS and RF Energy Transfer," *IEEE Trans. Wirel. Commun.*, vol. 13, no. 5, pp. 2646–2658, May 2014.
[22] H. Lee, S. Lee, K. Lee, H. Kong, and I. Lee, "Optimal Beamforming Designs for Wireless Information and Power Transfer in MISO Interference Channels," *IEEE Trans. Wirel. Commun.*, vol. 14, no. 9, pp. 4810–4821, Sep. 2015.
[23] C. Song, J. Park, B. Clerckx, I. Lee, and K. Lee, "Generalized Precoder Designs Based on Weighted MMSE Criterion for Energy Harvesting Constrained MIMO and Multi-User MIMO Channels," *IEEE Trans. Wirel. Commun.*, vol. 15, no. 12, pp. 7941–7954, Dec. 2016.
[24] A. A. Nasir, H. D. Tuan, D. T. Ngo, T. Q. Duong, and H. V. Poor, "Beamforming Design for Wireless Information and Power Transfer Systems: Receive Power-Splitting Versus Transmit Time-Switching," *IEEE Trans. Commun.*, vol. 65, no. 2, pp. 876–889, Feb. 2017.
[25] J. Kang, I. Kim, and D. I. Kim, "Joint Tx Power Allocation and Rx Power Splitting for SWIPT System With Multiple Nonlinear Energy Harvesting Circuits," *IEEE Wirel. Commun. Lett.*, vol. 8, no. 1, pp. 53–56, Feb. 2019.
[26] C. Song and Y. Jeon, "Weighted MMSE Precoder Designs for Sum-Utility Maximization in Multi-User SWIPT Network-MIMO With Per-BS Power Constraints," *IEEE Trans. Veh. Technol.*, vol. 67, no. 3, pp. 2809–2813, Mar. 2018.
[27] C. Song, H. Lee, and K. Lee, "Optimal Precoder Designs for Sum-Utility Maximization in SWIPT-Enabled Multi-User MIMO Cognitive Radio Networks," *IEEE Syst. J.*, vol. 13, no. 3, pp. 2332–2343, Sep. 2019.
[28] L. Liu, R. Zhang, and K. Chua, "Wireless Information and Power Transfer: A Dynamic Power Splitting Approach," *IEEE Trans. Commun.*, vol. 61, no. 9, pp. 3990–4001, Sep. 2013.
[29] X. Zhou, R. Zhang, and C. K. Ho, "Wireless Information and Power Transfer: Architecture Design and Rate-Energy Tradeoff," *IEEE Trans. Commun.*, vol. 61, no. 11, pp. 4754–4767, Nov. 2013.
[30] W. Lu, W. Zhao, S. Hu, X. Liu, B. Li, and Y. Gong, "OFDM Based SWIPT for Two-Way AF Relaying Network," *IEEE Access*, vol. 6, pp. 73 223–73 231, 2018.
[31] H. Lee, K. Lee, H. Kim, and I. Lee, "Joint Transceiver Optimization for MISO SWIPT Systems With Time Switching," *IEEE Trans. Wirel. Commun.*, vol. 17, no. 5, pp. 3298–3312, May 2018.
[32] B. Clerckx, "Wireless Information and Power Transfer: Nonlinearity, Waveform Design, and Rate-Energy Tradeoff," *IEEE Trans. Signal Process.*, vol. 66, no. 4, pp. 847–862, Feb. 2018.
[33] G. Ma, J. Xu, Y. Zeng, and M. R. V. Moghadam, "A Generic Receiver Architecture for MIMO Wireless Power Transfer With Nonlinear Energy Harvesting," *IEEE Signal Process. Lett.*, vol. 26, no. 2, pp. 312–316, Feb. 2019.
[34] H. Sampath, S. Talwar, J. Tellado, V. Erceg, and A. Paulraj, "A fourth-generation MIMO-OFDM broadband wireless system: Design, performance, and field trial results," *IEEE Commun. Mag.*, vol. 40, no. 9, pp. 143–149, Sep. 2002.
[35] T. S. Rappaport, A. Annamalai, R. M. Buehrer, and W. H. Tranter, "Wireless communications: Past events and a future perspective," *IEEE Commun. Mag.*, vol. 40, no. 5, pp. 148–161, May 2002.
[36] T. A. Weiss and F. K. Jondral, "Spectrum pooling: An innovative strategy for the enhancement of spectrum efficiency," *IEEE Commun. Mag.*, vol. 42, no. 3, pp. S8–14, Mar. 2004.
[37] A. Ikhlef, "Optimal MIMO Multicast Transceiver Design for Simultaneous Information and Power Transfer," *IEEE Commun. Lett.*, vol. 18, no. 12, pp. 2153–2156, Dec. 2014.
[38] T. K. Lyu, "Capacity of multi-user MIMO systems with MMSE and ZF precoding," in *2016 IEEE Conference on Computer Communications Workshops (INFOCOM WKSHPS)*, Apr. 2016, pp. 1083–1084.
[39] Z. Na, X. Li, X. Liu, and Z. Deng, "Subcarrier allocation based simultaneous wireless information and power transfer for multiuser OFDM systems," *J Wireless Com Network*, vol. 2017, no. 1, p. 148, Sep. 2017.
[40] X. Wang, S. Ekin, and E. Serpedin, "Optimal resource allocation for downlink OFDM-Based cognitive radio networks," in *2017 International Symposium on Networks, Computers and Communications (ISNCC)*, May 2017, pp. 1–6.
[41] J. Brehmer, *Utility Maximization in Nonconvex Wireless Systems*, ser. Foundations in Signal Processing, Communications and Networking. Berlin: Springer, 2012, no. 5.
[42] Wei Yu and R. Lui, "Dual methods for nonconvex spectrum optimization of multicarrier systems," *IEEE Trans. Commun.*, vol. 54, no. 7, pp. 1310–1322, Jan. 2006.
[43] Z. Luo and S. Zhang, "Dynamic Spectrum Management: Complexity and Duality," *IEEE J. Sel. Top. Signal Process.*, vol. 2, no. 1, pp. 57–73, Feb. 2008.
[44] I. C. Wong and B. L. Evans, "OFDMA Downlink Resource Allocation for Ergodic Capacity Maximization with Imperfect Channel Knowledge," *IEEE GLOBECOM 2007 - IEEE Glob. Telecommun. Conf.*, pp. 3729–3733, Nov. 2007.

[45] M. K. Awad, V. Mahinthan, M. Mehrjoo, X. Shen, and J. W. Mark, "A Dual-Decomposition-Based Resource Allocation for OFDMA Networks With Imperfect CSI," *IEEE Trans. Veh. Technol.*, vol. 59, no. 5, pp. 2394–2403, Jun. 2010.

[46] Z. Luo and S. Zhang, "Duality Gap Estimation and Polynomial Time Approximation for Optimal Spectrum Management," *IEEE Trans. Signal Process.*, vol. 57, no. 7, pp. 2675–2689, Jul. 2009.

[47] R. Hunger, M. Joham, and W. Utschick, "On the MSE-Duality of the Broadcast Channel and the Multiple Access Channel," *IEEE Trans. Signal Process.*, vol. 57, no. 2, pp. 698–713, Feb. 2009.

[48] D. Tse and P. Viswanath, *Fundamentals of Wireless Communication*. Cambridge University Press, 2005.

[49] M. Razaviyayn, M. Hong, and Z.-Q. Luo, "A Unified Convergence Analysis of Block Successive Minimization Methods for Nonsmooth Optimization," *SIAM J. Optim.*, vol. 23, no. 2, pp. 1126–1153, Jan. 2013.

[50] G. Scutari, F. Facchinei, P. Song, D. P. Palomar, and J.-S. Pang, "Decomposition by Partial Linearization: Parallel Optimization of Multi-Agent Systems," *IEEE Trans. Signal Process.*, vol. 62, no. 3, pp. 641–656, Feb. 2014.

[51] S. Rebennack, "Ellipsoid Method," in *Encyclopedia of Optimization*, C. A. Floudas and P. M. Pardalos, Eds. Boston, MA: Springer US, 2009, pp. 890–899.

[52] M. Grötschel, L. Lovász, and A. Schrijver, *Geometric Algorithms and Combinatorial Optimization*, ser. Algorithms and Combinatorics. Springer, 1988, no. 2.

[53] R. G. Bland, D. Goldfarb, and M. J. Todd, "Feature Article—The Ellipsoid Method: A Survey," *Oper. Res.*, vol. 29, no. 6, pp. 1039–1091, Dec. 1981.

[54] K. T. Abou–Moustafa, "On Derivatives of Eigenvalues and Eigenvectors of the Generalized Eigenvalue Problem," Centre of Intelligent Machines, McGill University, Montréal, Canada, Tech. Rep. TR–CIM–10–10, 2010.

[55] J. Verdyck, W. Lanneer, P. Tsiaflakis, W. Coomans, P. Patrinos, and M. Moonen, "Optimal Dynamic Spectrum Management Algorithms for Multi-User Full-Duplex DSL," *IEEE Access*, vol. 7, pp. 106 600–106 616, 2019.

[56] J. Verdyck and M. Moonen, "Dynamic Spectrum Management in Digital Subscriber Line Networks With Unequal Error Protection Requirements," *IEEE Access*, vol. 5, pp. 18 107–18 120, 2017.

[57] H. Hijazi, L. Ros, and G. Jourdain, "OFDM Channel Parameters Estimation used for ICI Reduction in time-varying Multipath Channels," in *European Wireless Conference*, Paris, France, Apr. 2007, p. 6 pages.

[58] E. Björnson, M. Bengtsson, and B. Ottersten, "Optimal Multiuser Transmit Beamforming: A Difficult Problem with a Simple Solution Structure [Lecture Notes]," *IEEE Signal Process. Mag.*, vol. 31, no. 4, pp. 142–148, Jul. 2014.

[59] Y. Huang and D. P. Palomar, "A Dual Perspective on Separable Semidefinite Programming With Applications to Optimal Downlink Beamforming," *IEEE Trans. Signal Process.*, vol. 58, no. 8, pp. 4254–4271, Aug. 2010.

[60] M. Grant and S. Boyd, "CVX: Matlab software for disciplined convex programming, version 2.1," Mar. 2014.

[61] ——, "Graph implementations for nonsmooth convex programs," in *Recent Advances in Learning and Control*, ser. Lecture Notes in Control and Information Sciences, V. Blondel, S. Boyd, and H. Kimura, Eds. Springer-Verlag Limited, 2008, pp. 95–110.



RICHARD P. KETCHAM (M'07) received a M.Sc. degree in electrical engineering in 2007 from the University of Vermont in Burlington, Vermont, USA. In 2007, he received the Cyril G. Veinott graduate award for excellence in performance and greatest promise of success. Between 2007 and 2018, he worked as an embedded systems engineer for MicroStrain Inc., which was acquired by LORD Corporation. In this position, he designed wireless sensing networks for use in various industrial applications. He received the Mountain Mover award in 2014 in recognition for his role in designing innovative tools used by Caterpillar Inc. In 2018, he began and continues to pursue a Ph.D. degree in electrical engineering at KU Leuven under the supervision of Prof. M. Moonen.



JEROEN VERDYCK (S'15) received the M.Sc. degree in electrical engineering from KU Leuven, Leuven, Belgium, in 2014, where he is currently pursuing the Ph.D. degree with the Electrical Engineering Department, under the supervision of Prof. M. Moonen. He is involved in joint projects with KU Leuven and University of Antwerp, Antwerp, Belgium. His research interests include signal processing and optimization for digital communication systems with an emphasis on DSL wireline access networks.



MARC MOONEN (M'94, SM'06, F'07) is a Full Professor at the Electrical Engineering Department of KU Leuven, where he is heading a research team working in the area of numerical algorithms and signal processing for digital communications, wireless communications, DSL and audio signal processing.

He is a Fellow of the IEEE (2007) and a Fellow of EURASIP (2018). He received the 1994 KU Leuven Research Council Award, the 1997 Alcatel Bell (Belgium) Award (with Piet Vandaele), the 2004 Alcatel Bell (Belgium) Award (with Raphael Cendrillon), and was a 1997 Laureate of the Belgium Royal Academy of Science. He received journal best paper awards from the IEEE Transactions on Signal Processing (with Geert Leus and with Daniele Giacobello) and from Elsevier Signal Processing (with Simon Doclo). He was chairman of the IEEE Benelux Signal Processing Chapter (1998-2002), a member of the IEEE Signal Processing Society Technical Committee on Signal Processing for Communications, and President of EURASIP (European Association for Signal Processing, 2007-2008 and 2011-2012). He is currently Vice-President for Publications of the IEEE Signal Processing Society (2021-2023).

He has served as Editor-in-Chief for the EURASIP Journal on Applied Signal Processing (2003-2005), Area Editor for Feature Articles in IEEE Signal Processing Magazine (2012-2014), and has been a member of the editorial board of Signal Processing, IEEE Transactions on Circuits and Systems II, IEEE Signal Processing Magazine, Integration-the VLSI Journal, EURASIP Journal on Wireless Communications and Networking and EURASIP Journal on Advances in Signal Processing.